Chapter

Advances in Dropwise Condensation: Dancing Droplets

Rongfu Wen and Xuehu Ma

Abstract

Vapor condensation is a ubiquitous phase change phenomenon in nature, as well as widely exploited in various industrial applications such as power generation, water treatment and harvesting, heating and cooling, environmental control, and thermal management of electronics. Condensation performance is highly dependent on the interfacial transport and its enhancement promises considerable savings in energy and resources. Recent advances in micro/nano-fabrication and surface chemistry modification techniques have not only enabled exciting interfacial phenomenon and condensation enhancement but also furthered the fundamental understanding of interfacial wetting and transport. In this chapter, we present an overview of dropwise condensation heat transfer with a focus on improving droplet behaviors through surface design and modification. We briefly summarize the basics of interfacial wetting and droplet dynamics in condensation process, discuss the underlying mechanisms of droplet manipulation for condensation enhancement, and introduce some emerging works to illustrate the power of surface modification. Finally, we conclude this chapter by providing the perspectives for future surface design in the field of condensation enhancement.

Keywords: condensation, micro/nanostructures, droplet, wetting, nucleation, heat transfer enhancement

1. Introduction

Condensation heat transfer has been at the forefront of both fundamental and engineering research due to its significance in many conventional and emerging industrial applications. For example, vapor condensation has been widely exploited for thermal management of high-power systems to maintain adequate performance and system reliability, such as advanced lasers, light-emitting diodes, radars, microprocessors, electrical machines, and power inverters [1, 2]. Meanwhile, the thermal efficiency of steam cycles, responsible for a major fraction of electricity production, is highly dependent on the heat transfer performance of vapor condensation [3]. Furthermore, condensation performance strongly influences the energy and infrastructure costs of water treatment and desalination technologies, which is becoming increasingly important due to water scarcity and world population growth [4]. Recent advances in condensation processes on the micro/nanostructured surfaces have also enabled many emerging applications in water and energy systems, such as atmospheric water harvesting [5], solar steam generation [6, 7], humidity control of building environment [8], droplet-jumping-induced gas

absorption [9], jumping-droplet electronics cooling [10, 11], and jumping-droplet electrostatic energy harvesting [12]. More natural phenomena and emerging applications in the field can be found in **Figure 1**.

Vapor preferentially condenses on a solid substrate rather than directly homogeneous nucleation in the vapor phase due to the smaller energy barrier [13]. Once vapor condensation occurs on a solid substrate, the wetting of liquid condensate, determined by surface topography and chemical compositions, plays a key role in heat transfer performance as it is involved in the whole cycle of nucleation, growth, and departure of a liquid phase [14]. Dropwise condensation on a hydrophobic surface, where the gravity-driven droplet roll-off frequently refresh the surface, has an order of magnitude higher heat transfer efficiency than that of filmwise condensation on a hydrophilic surface, where a continuously thickening liquid film covers on the condensing surface [15]. Dropwise condensation is an intrinsically multi-scale energy transfer process, involving the initial formation of droplets at a length scale at a few nanometers, then growth and coalescence, and final droplet departure/shedding of at the millimeter scale, as shown in **Figure 2**. Besides, each sub-process of condensation has different preferred wettability for accelerating the whole cycle of condensed droplets, for example, easier initial nucleation on a hydrophilic substrate with low energy barrier, and faster surface refreshing on a hydrophobic surface with low surface adhesion [16–19]. Thus, the requirements on the surface topography and chemical compositions are dynamically varying from the initial nucleation to final droplet departure.

Despite that superhydrophobic surfaces with micro/nanostructures can further promote surface refreshing with spectacular water repellency, for example, self-propelled droplet jumping, the presence of vapor layer within the micro/nanostructures that is beneficial for reduce solid-liquid adhesion, brings in an additional thermal resistance to hinder droplet growth [20, 21]. Even worse is that the nucleation of nanoscale droplets within micro/nanostructures can cause unwanted pinned states of condensed droplets, which can lead to flooding phenomenon and ultimately heat transfer degradation of superhydrophobic surfaces [22–26]. To

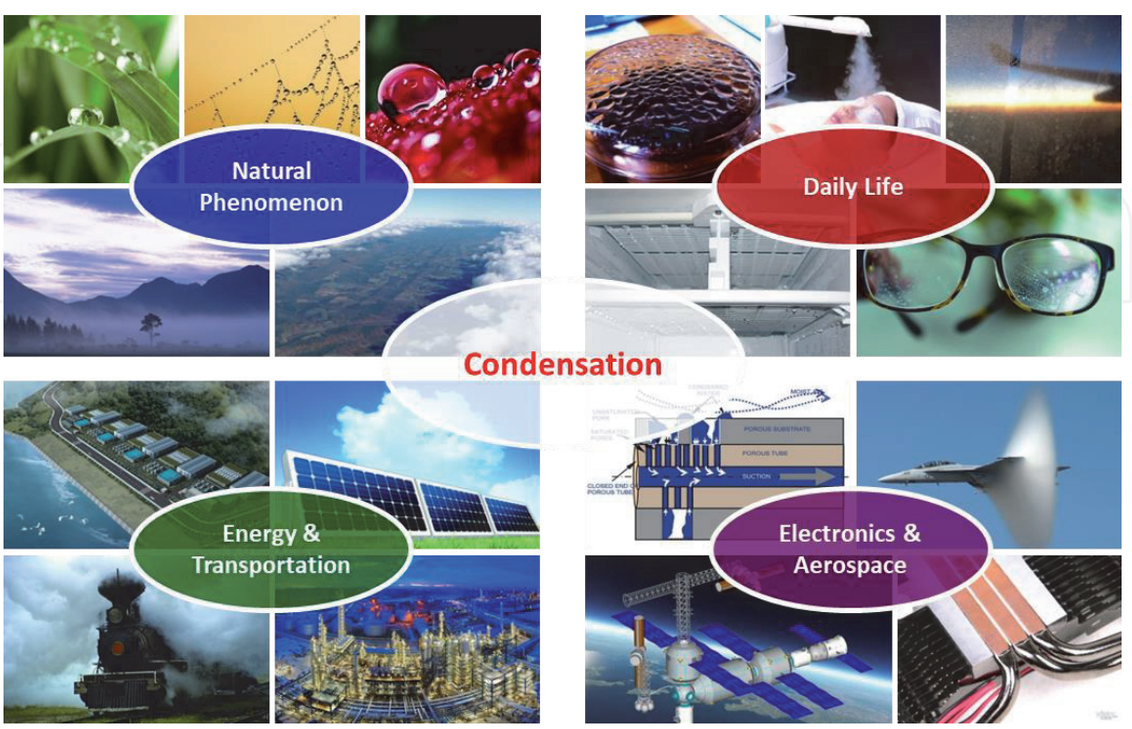

Figure 1.
Condensation phenomenon in nature and daily lives, and its applications in various conventional and emerging industrial systems. The high efficiency of vapor condensation heat transfer is critical in water and energy fields.

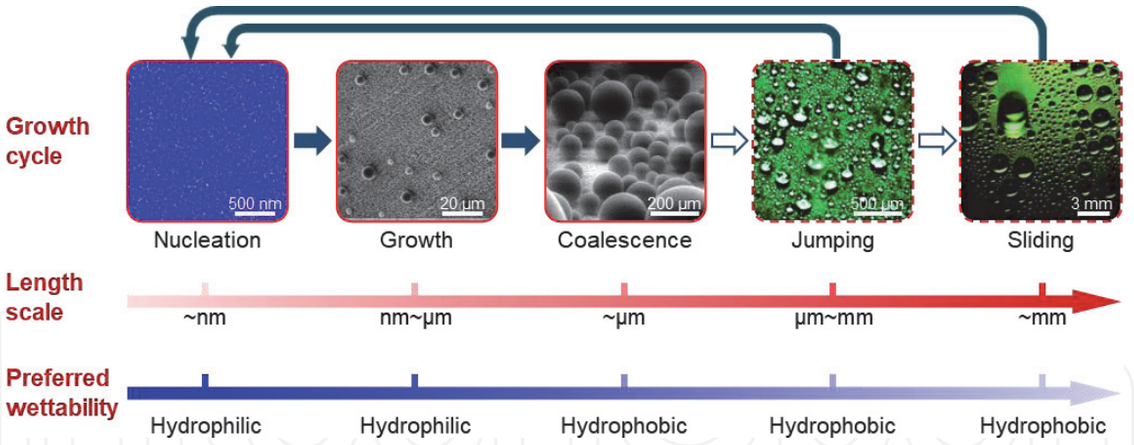

Figure 2.
Multiscale characteristics of dropwise condensation and differential preference on wettability for various subprocesses. Droplet cycle from nucleation to departure has the characteristic length scales from a few nanometers to several millimeters and the preferred wettability from hydrophilicity to hydrophobicity.

prevent the nucleation-induced flooding, some emerging techniques, for example, hybrid surfaces with wettability contrast and slippery liquid-infused porous (SLIP) surfaces, have been proposed to manipulate droplet behaviors in condensation process. For example, the different wettability on a hybrid surface can spatially control initial nucleation, addressing the random nucleation on a uniform surface [18, 19, 27]. On a SLIP surface, the lubricating fluid is immiscible with liquid condensate while preferentially wets the micro/nanostructures on the substrate, creating a lubricating fluid layer between the substrate and condensed droplets to reduce surface adhesion for high droplet mobility [5, 28–30].

Given the importance of surface structures and wettability on condensation processes, intensive efforts have been devoted to understanding the physics of dropwise condensation and to developing various micro/nanostructures and functional coatings to control droplet behaviors. In this chapter, we present an overview of the advance in dropwise condensation with a focus on improving droplet dynamics by surface modification. We briefly summarize the surface fabrication and modification, introduce droplet nucleation and size distribution in dropwise condensation, discuss the underlying mechanisms of droplet manipulation using micro/nanostructures, and introduce some typical works to illustrate the power of surface modification. We also discuss several emerging strategies to enhance condensation that could break the limit of conventional dropwise condensation. Finally, we conclude this chapter by providing the perspectives for future surface design in the field of condensation enhancement.

2. Basics of dropwise condensation

Wetting behavior of liquid condensate on the substrate is critical in condensation process. For a smooth surface without roughness, a droplet forms an intrinsic contact angle, defined as the angle between the solid-liquid and liquid-vapor interfaces within the liquid (**Figure 3**). The intrinsic contact angle θ is a force balance at the tri-phase contact line, which can be described by the Young equation,

$$\sigma_{lv} \cos\theta = \sigma_{sv} - \sigma_{sl} \tag{1}$$

where σ_{lv}, σ_{sv}, and σ_{sl} are the liquid-vapor, solid-vapor, and solid-liquid interfacial tensions, respectively. On a real surface with roughness, there is a contact angle

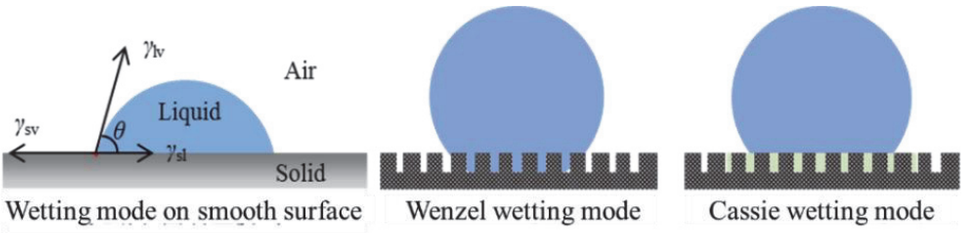

Figure 3.
Wetting states of a droplet on the smooth and structured surfaces. Intrinsic contact angle of a droplet on a smooth surface and apparent contact angle of a droplet in Wenzel and Cassie states on a structured surface.

hysteresis for an incipient droplet motion $\Delta\theta$, defined as the difference between advancing contact angle θ_{adv} and receding contact angle θ_{rec}. When a water contact angle on a surface is typically smaller or larger than 90°, the surface is defined as hydrophilic or hydrophobic, respectively. Further introducing the roughness, for example, micro/nanostructures, can increase surface hydrophobicity to superhydrophobicity, defined with a contact angle larger than 150° and a contact angle hysteresis smaller than 5° [31].

During condensation process, the wetting of condensed droplets on a rough surface can be differentiated into the highly pinned Wenzel state with large adhesion and suspended Cassie state with high mobility. Both Wenzel and Cassie states can be understood as a global energy minimization of a droplet. On such a surface with roughness r defined as the ratio of the total surface area to projected area, the apparent contact angle of a droplet in Wenzel state can be expressed as,

$$\cos\theta_W = r\cos\theta \tag{2}$$

For a droplet in Cassie state on a rough surface, the apparent contact angle is defined by,

$$\cos\theta_C = \varphi(\cos\theta + 1) - 1 \tag{3}$$

Nucleation is the first step in dropwise condensation to create a new solid-liquid interface, followed by droplet growth and shedding [16]. The critical nucleation radius r_{min} is determined by both liquid properties and surface subcooling and it can be given by the classical nucleation equation [32],

$$r_{min} = \frac{2\sigma_{lv}T}{\rho_l h_{fg}\Delta T} \tag{4}$$

where ρ_l and h_{fg} are the liquid density and latent heat of the vapor-to-liquid phase transition, respectively. The energy barrier ΔG_e for droplet formation on a substrate should be overcome to activate the nucleation process [19],

$$\Delta G_e = \frac{\pi\sigma_{lv}r_{min}^2(2 - 3\cos\theta + \cos^3\theta)}{3} \tag{5}$$

Compared to a hydrophobic surface with a larger contact angle θ, vapor nucleation occurs more easily on a hydrophilic surface with a smaller intrinsic contact angle. The intrinsic wettability of a surface also has a strong effect on the nucleation rate J via the inverse exponential dependence on ΔG_e [19],

$$J = J_0 \exp\left(-\frac{\Delta G_e}{kT}\right) = J_0 \exp\left(-\frac{\pi\sigma_{lv}r_{min}^2(2 - 3\cos\theta + \cos^3\theta)}{kT}\right) \tag{6}$$

where J_0 is a kinetic constant. Once a droplet nucleates on the surface, it grows by direct vapor-to-liquid condensation on the droplet surface. During initial growth without coalescence, droplets grow with an expected radius as a function of time as,

$$R = t^{\alpha} \tag{7}$$

where α is the power-law exponent, which ranges from 0 to 1 depending on the surface property, surface subcooling, and vapor conditions. If non-condensable gas (NCG) is present in the vapor, a mass transfer boundary layer will be established near the solid surface, resulting in vapor molecules diffusion through the boundary layer to the droplet surface. The mass transfer flux can be expressed as,

$$w = D_{12}\frac{(p_r - p_s)}{\delta_0 RT} \tag{8}$$

where D_{12} is the diffusion constant of vapor molecules in the gas. p_{r} and p_{s} are the vapor pressure and saturation pressure, respectively. δ_0 is the thickness of the boundary layer. Here, the boundary layer thickness can be related to the free-stream velocity U, the kinematic viscosity μ, and the Schmidt number, $\mathrm{Sc} = \mu/D_{12}$, by

$$\delta_0 = \frac{(x\mu/U)^{1/2}}{CSc^{1/3}} \tag{9}$$

When a droplet grows large enough to contact with adjacent droplets, they merge and speed up droplet growth, stabilizing the surface coverage to a constant value, known as the self-similarity in dropwise condensation [14, 15, 17, 33, 34]. On a vertical or inclined hydrophobic surface, condensed droplets are generally removed by the gravity-driven shedding. Droplet departure radius $r_{\max}$ can thus be estimated by the force balance between the surface tension and gravity [35],

$$r_{\max} = \left(\frac{6\mathrm{c}(\cos\theta_{\mathrm{rec}} - \cos\theta_{\mathrm{adv}})\sin\theta}{\pi(2 - 3\cos\theta + \cos^3\theta)}\frac{\sigma_{\mathrm{lv}}}{\rho_{\mathrm{l}}g}\right)^{1/2} \tag{10}$$

Once the droplets begin to departure from the surface driven by the gravity, other droplets in the path of droplet departure can be effectively swept by coalescence, refreshing the condensing surface. New small droplets then re-nucleate, grow, and coalescence on the fresh surface, which is responsible for the high-efficiency heat transfer performance of dropwise condensation [36, 37]. Compared with the time scale of initial nucleation, the duration of droplet growth, coalescence, and departure usually dominates the whole cycle [1, 37]. Increasing apparent contact angle θ and decreasing contact angle hysteresis ($\theta_{\mathrm{adv}} - \theta_{\mathrm{rec}}$) can effectively reduce droplet departure size for accelerating surface refreshing.

Understanding the cycle of condensed droplets on a solid surface, a classical model was proposed by Le Fevre and Rose to predict dropwise condensation heat transfer where the heat transfer through individual droplet is calculated first and the average heat flux is then obtained by integrating over all the distributed droplets on the condensing surface [38].

$$q = \int_{r_{\min}}^{r_{\max}} q_{\mathrm{d}}(r)N(r)\mathrm{d}r \tag{11}$$

where q_{d} is the heat flux through an individual droplet and N is the droplet size distribution on the surface. Subsequently, corresponding modifications of dropwise

condensation heat transfer model to include more accurate expressions for the heat transfer through an individual droplet [35, 39–48] and droplet size distribution [14, 33, 39, 43, 46, 49–51] are developed, for example, the conduction resistance of the liquid droplet, the thermal resistance of a hydrophobic coating, mass transfer on the liquid–vapor interface, and the effect of interface curvature.

3. Surface fabrication for dropwise condensation

In most thermal systems, liquid condensate typically forms a liquid film on the heat transfer surface because of the high surface energy of common industrial components such as clean metals. To achieve dropwise condensation for high-efficient heat transfer, various hydrophobic coatings such as long-chain fatty acid, polymer materials, rare-earth oxide ceramics, and self-assembled monolayers [14, 37, 52–58], are usually applied to increase hydrophobicity for high water repellency. Monolayer coatings, typically a few nanometers in thickness, for example, long-chain fluorocarbons and fatty acids, can increase water repellency of the surface with a negligible additional thermal resistance (**Figure 4a**). However, they are generally not durable due to the low chemical stability and low bonding strength with the substrate [14, 52]. With a similar hydrophobicity, polytetrafluoroethylene (PTFE) coatings have been attempted to increase surface repellency while maintaining low thermal resistance (**Figure 4b**) [59]. Thicker polymer coatings have been shown to maintain robust water repellency during vapor condensation (**Figure 4c**). However, they typically have a large thermal resistance that can even negate the heat transfer enhancement achieved by dropwise condensation [54]. In addition, the initiated chemical vapor deposition (iCVD) and plasma-enhanced CVD techniques have been used to grow ultrathin conformal polymer coatings to achieve hydrophobicity (**Figure 4d**). However, further study is necessary to evaluate the durability of these ultrathin coatings for condensation heat transfer enhancement [55, 58]. Recently, ultrathin graphene (**Figure 4e**) with low thermal

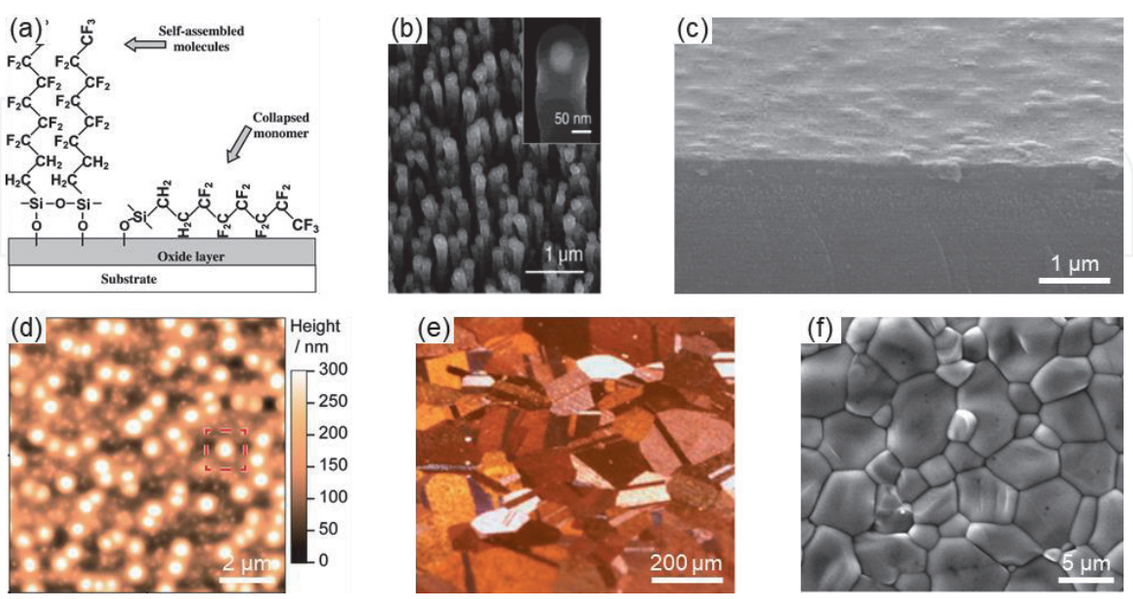

Figure 4.
Hydrophobic coatings for achieving dropwise condensation. (a) Self-assembled monolayer coating [52]. (b) Polytetrafluoroethylene (PTFE) coating on carbon nanotubes [53]. (c) Fluorocarbon film from perfluorocyclobutane precursors [54]. (d) Thin film of poly-(1H,1H,2H,2H-perfluorodecyl acrylate)-co-divinyl benzene p(PFDA-co-DVB) grafted to a substrate by iCVD [55]. (e) Graphene coatings on copper substrate [56]. (f) Rare-earth oxide ceramics [57].

resistance and good chemical stability has been used to obtain stable dropwise condensation, without obvious heat transfer degradation in a 2-week measurement [56]. Another typical material is the rare-earth oxide (REO), which can be potentially used as a hydrophobic material at scale due to the development of ceramic processing techniques (**Figure 4f**) [57]. Note that the wettability of REO is reported to be intrinsically hydrophilic and the hydrophobicity of REO is due to the adsorbed hydrocarbon species [60–62]. Despite that many new functional coatings mentioned above have shown some potential to achieve dropwise condensation, a cost-effective, low-thermal resistance, and robust hydrophobic coating to promote sustainable dropwise condensation has proven to be exceedingly challenging, resulting in ubiquitous filmwise condensation in real industrial applications.

To further improve droplet mobility, various micro/nanostructured surfaces are developed using advanced fabrication technologies. Micro/nanostructured silicon surfaces are fabricated using both wet and dry etching methods [69]. Typically, silicon nanowires synthesized by wet etching methods are vertically aligned [70]. Due to the surface tension of water during the drying process of nanowire synthesis, a large number of micro-defects are naturally formed where the closely aligned silicon nanowires cannot individually stand but form clusters [66]. Compared with the wet etching methods, finer structure geometries can be fabricated by dry etching where the etching rate can be controlled more precisely. In addition to the nanowires with uniform diameters, conical silicon nanowires were also fabricated to promote the formation of high-mobility droplets with the auxiliary Laplace pressure difference (**Figure 5a**) [25]. To meet the need of multiple length scales in manipulating droplet growth, hierarchical silicon nanowires with both microscale and nanoscale features have been fabricated by coupling micro-patterns and nanostructures [71]. **Figure 5b** shows a hierarchical surface with parallel microgrooves that are formed by patterning silicon nanowire arrays with different lengths [63, 72]. **Figure 5c** shows another hierarchical surface, consisting of micropyramids covered by silicon nanowires [64]. Compared to the silicon, metal materials, for example, aluminum, stainless steel, and copper, have better physical and thermal properties, to be exploited for improving heat transfer such as high thermal conductivity, stability, and machinability. Among various surface fabrication

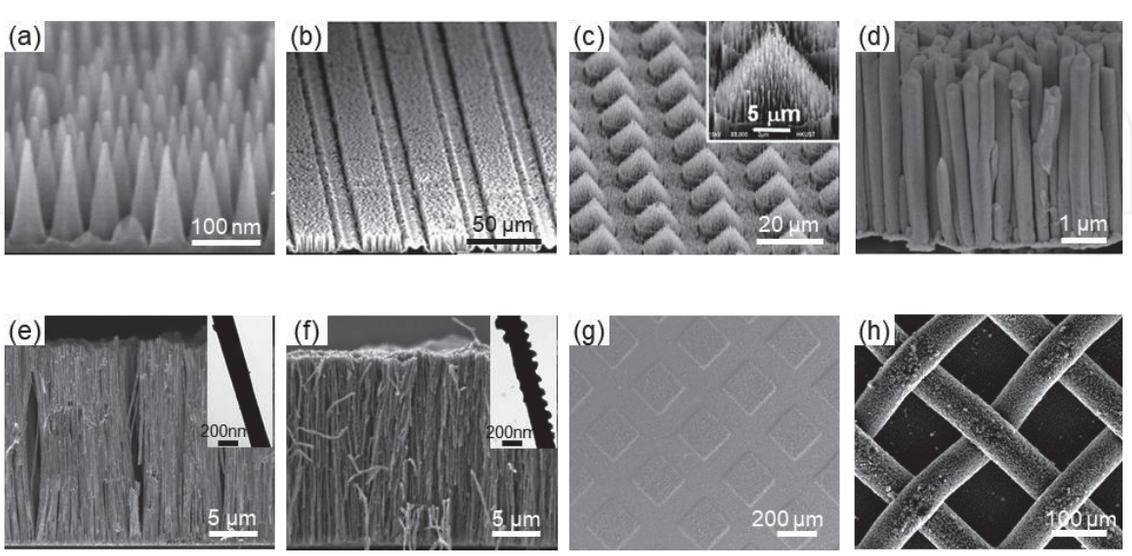

Figure 5.
Micro/nanostructured surfaces for condensation enhancement. (a) Conical silicon nanowire arrays [25]. (b) Microgroove silicon nanowires [63]. (c) Micro-pyramids covered by silicon nanowires [64]. (d) Gold nanowires [65]. (e) Closely spaced copper nanowire arrays [66]. (f) 3D copper nanowire networks [67]. (g) Hierarchical surface with micro-patterned copper nanowire arrays [21]. (h) Hierarchical copper mesh-covered structure [68].

methods for metal micro/nanostructures, the electrochemical deposition (or electroplating) method with the assistance of templates is considered to be a convenient and versatile approach [21, 65–67, 73]. **Figure 5d** shows the gold nanowires fabricated to promote droplet coalescence without direct coalescence [65]. Using a two-step template-assisted electrochemical deposition method, closely spaced copper nanowires were fabricated to promote the formation of mobile droplets in suspended wetting states (**Figure 5e**) [66]. To prevent the formation of microdefects between agglomerated nanowire arrays, the 3D copper nanowire networks consisting of interconnected nanowires with nanoscale bumps were fabricated using 3D porous anodic alumina oxide templates (**Figure 5f**). These nanobumps on the nanowire walls serve as anchors to fix adjacent nanowires [67]. **Figure 5g** shows a hierarchical surface with micro-patterned copper nanowire arrays [21]. In addition, the commercial metal materials, such as copper mesh, foam, and particles, have been applied to develop low-cost superhydrophobic surfaces and to provide a solution for large-scale deployment of enhanced heat transfer surfaces in a diverse range of technologies (**Figure 5h**) [68]. Despite that diverse micro/nanostructured surfaces have been fabricated to meet the multiple length scale need in manipulating droplet growth as mentioned above, there remains a need for advanced surface features to optimize droplet behaviors for future vapor condensation enhancement.

4. Nucleation and droplet size distribution

According to the classic nucleation theory, a substrate with low contact angles can decrease energy barrier and increase nucleation rate. The geometrical structure can also enable spatial distribution of nucleation sites on a micro/nanostructured surface. More interestingly, the structure feature plays an important role in determining the wetting mode of a nucleated droplet and subsequent droplet growth and dynamics. For example, a droplet in Cassie state has low adhesion and high mobility, which is favorable for dropwise condensation. Various theoretical and semiempirical models have been proposed to describe the relationship between surface structure and nucleation, for example, interfacial free energy analysis and cluster theory [16, 17, 19, 74]. To obtain more detailed information on the droplet nucleation in micro/nanostructures, many numerical modeling methods have been developed such as the Gibbs free energy analyses, finite element method, lattice Boltzmann method, lattice density functional method, and molecular dynamics (MD) simulations [13, 18, 75–80].

Nucleation of water droplet on the surfaces with different wettability and structural features has been widely investigated by MD simulations. The nucleation process and wetting state of nucleated droplets were obtained by manipulating the interaction potentials between surface atoms and vapor molecules [13]. The near-constant contact angles can be established for nanoscale nucleated droplets on a surface, decreasing as the solid-liquid interaction intensities linearly. On an uniform high-energy surface (**Figure 6a**), the interactions between surface atoms and water molecules are strong to capture water molecules rapidly once they get close to the surface. A large number of water molecules are absorbed on the surface and the nucleation occurs almost instantaneously. On a hybrid surface with different surface energies (**Figure 6b**), where high-energy sites distributed on a low-surface energy surface, the nucleation preferably initiates on the high-energy sites. The clusters are trapped on the high-energy sites instead of migrating around observed on an uniform surface (**Figure 6a**). The growth of nucleated droplets on high-energy particles can be divided into three stages: the formation of a wet-spot,

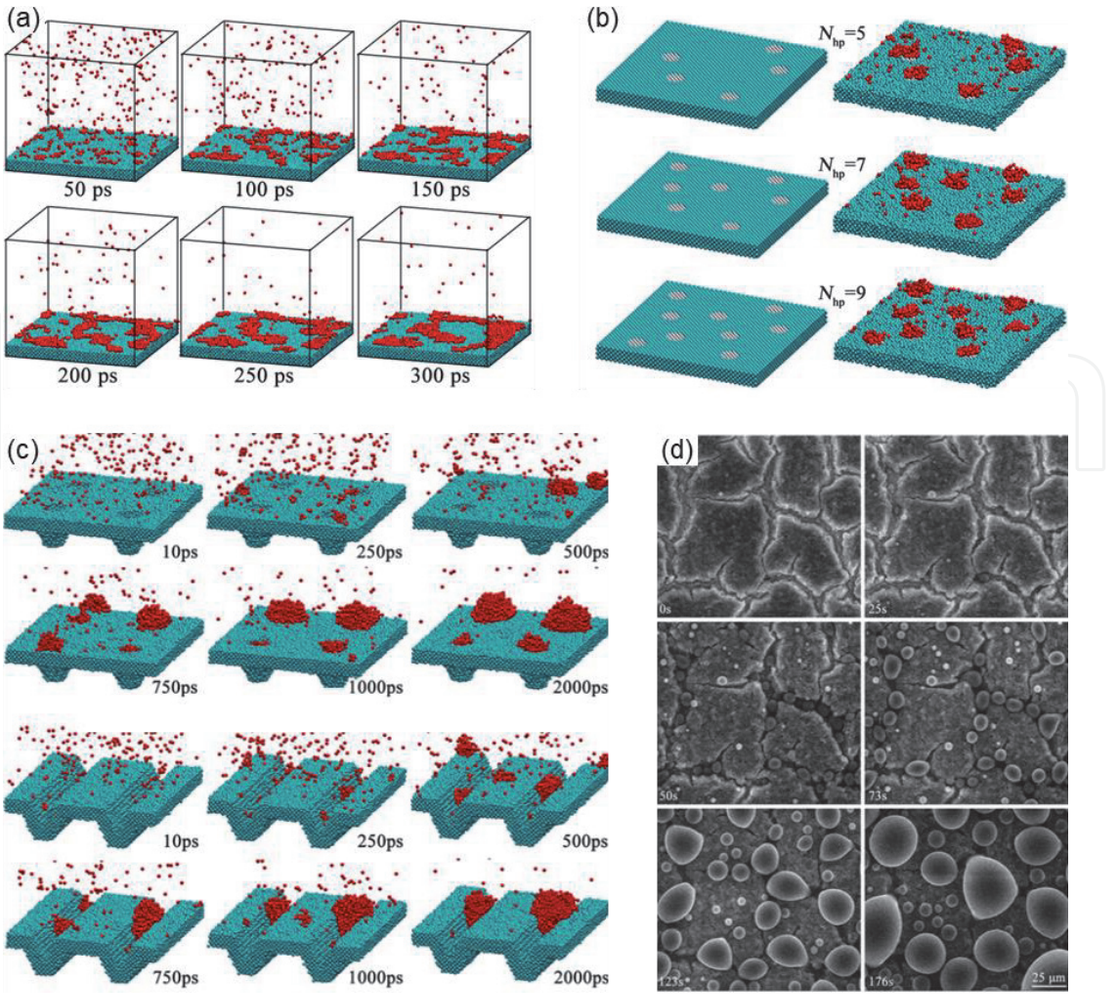

Figure 6.
Effect of surface energy and structure feature on the nucleation. (a) Random nucleation occurring on a uniform smooth surface. (b) Initial nucleation occurs selectively in the high-energy sites on the hybrid surfaces with wetting contrast [13]. (c) Effect of structure features (micropores and microgrooves) on the initial nucleation. (d) ESME images showing droplets prefer to nucleate in the micro-defects on a nanostructured surface.

increase of contact angle with near-constant contact line, and finally growth with constant contact angle. The droplet growth rate can be improved by increasing the size of high-energy sites. Moreover, the microstructures (**Figure 6c**), for example, micro-pores and microgrooves, can promote droplet nucleation due to the lower energy barrier caused by the larger solid-liquid contact area when compared with a smooth surface. The preferred nucleation in the microstructures was also observed on the nanostructured surfaces with micro-defects (**Figure 6d**).

After droplets nucleate on a solid surface, they can grow through two mechanisms: direct growth without coalescence for the small droplets by vapor condensing on the liquid-vapor interface, and coalescence-dominated growth for the large droplets by merging with neighboring droplets. As a result, condensed droplets with a wide range of sizes exist on a surface, forming a unique self-similarity. The transient characteristic of droplet size distribution has been widely studied to understand the heat transfer mechanism of dropwise condensation [14, 17, 32, 34, 51, 81, 82]. In the initial droplet growth stage after nucleation, all the droplet sizes are uniform and droplet size distribution has a peak value, showing the lognormal distribution (**Figure 7a**). With droplets growing up, the average droplet size increases. Then, the coalescences among droplets lead to a wider span of droplet size and decline of the right peak. With the increasing space among the first generation droplets, new droplets nucleate and grow at the exposed substrate, forming a bimodal distribution. With further coalescence and nucleation, the

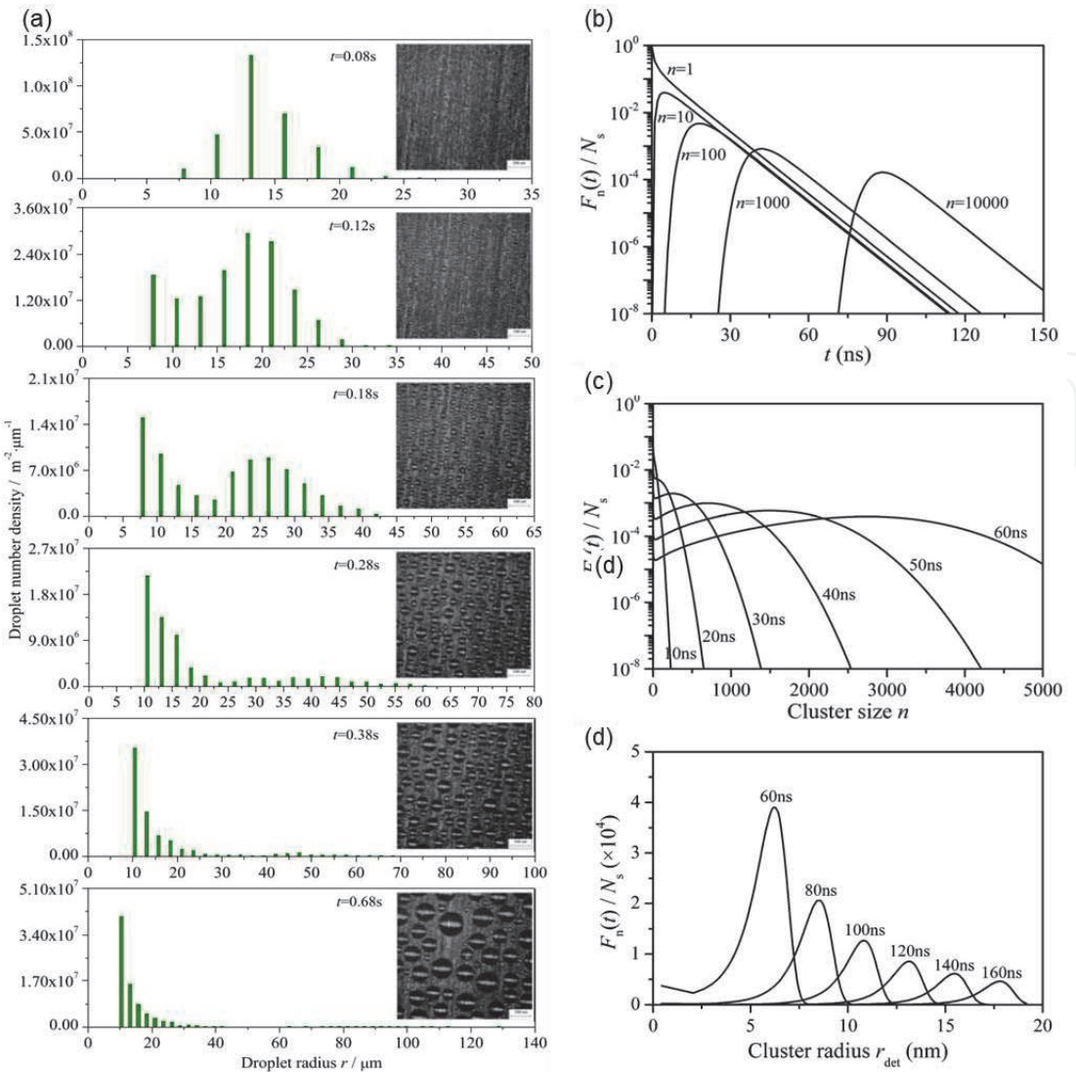

Figure 7.
Evolution of droplet size distribution on a plain hydrophobic surface. (a) Experimental results of the transient droplet size distribution in condensation [14]. (b–d) Evolution of cluster size distribution by MD simulation: (b) cluster size distribution as a function of time, (c) cluster size distribution as a function of time by MD simulation and (d) evolution of cluster radius distribution [17].

number of larger droplets decreases while the number of smaller droplets increases, and droplet size range becomes wider. Finally, the right peak vanishes and the distribution becomes unimodal. Due to the self-similarity feature of droplet size distribution, a representative large enough surface area contains various growth stages, resulting in a steady-state droplet size distribution [14, 82].

To further understand the evolution of droplet size distribution, a transient cluster size distribution model was introduced to investigate the kinetics of the initial condensation stage by MD simulation method [17]. It is well known that the growth/decay of clusters is significantly affected by the cluster size and contact angles of the condensing surface. With the increase of cluster sizes, more surface area of the cluster is exposed to the vapor, as well as the increased attachment/detachment frequencies. When the contact angle decreased to a certain value, the attachment frequency becomes larger than detachment frequency, resulting in the continuous growth of the clusters and subsequent nucleation. The results of the evolution of cluster/droplet size distribution indicate that the transient cluster size distribution translates from a monotonic decreasing distribution to a unimodal distribution with time (**Figure 7b,c**). The cluster radius at the peak of cluster/droplet size distribution curve shifts to the larger cluster sizes with time. However,

the peak value decreases as the size distribution curve is close to a lognormal distribution with time, which is distinctly different from the homogeneous equilibrium distribution (**Figure 7d**).

5. Condensation on superhydrophobic surfaces

Surface modification plays a crucial role in manipulating droplet wetting and dynamics. When micro/nanostructures are covered with hydrophobic coatings, the resulted superhydrophobic surfaces can promote the formation of highly mobile droplets in the Cassie states. More interestingly, it has been demonstrated that on such micro/nanostructured superhydrophobic surfaces small microdroplets can undergo coalescence-induced droplet jumping due to the release of excess surface energy (**Figure 8a**), which is independent of gravity [75, 76, 83, 84]. Jumping

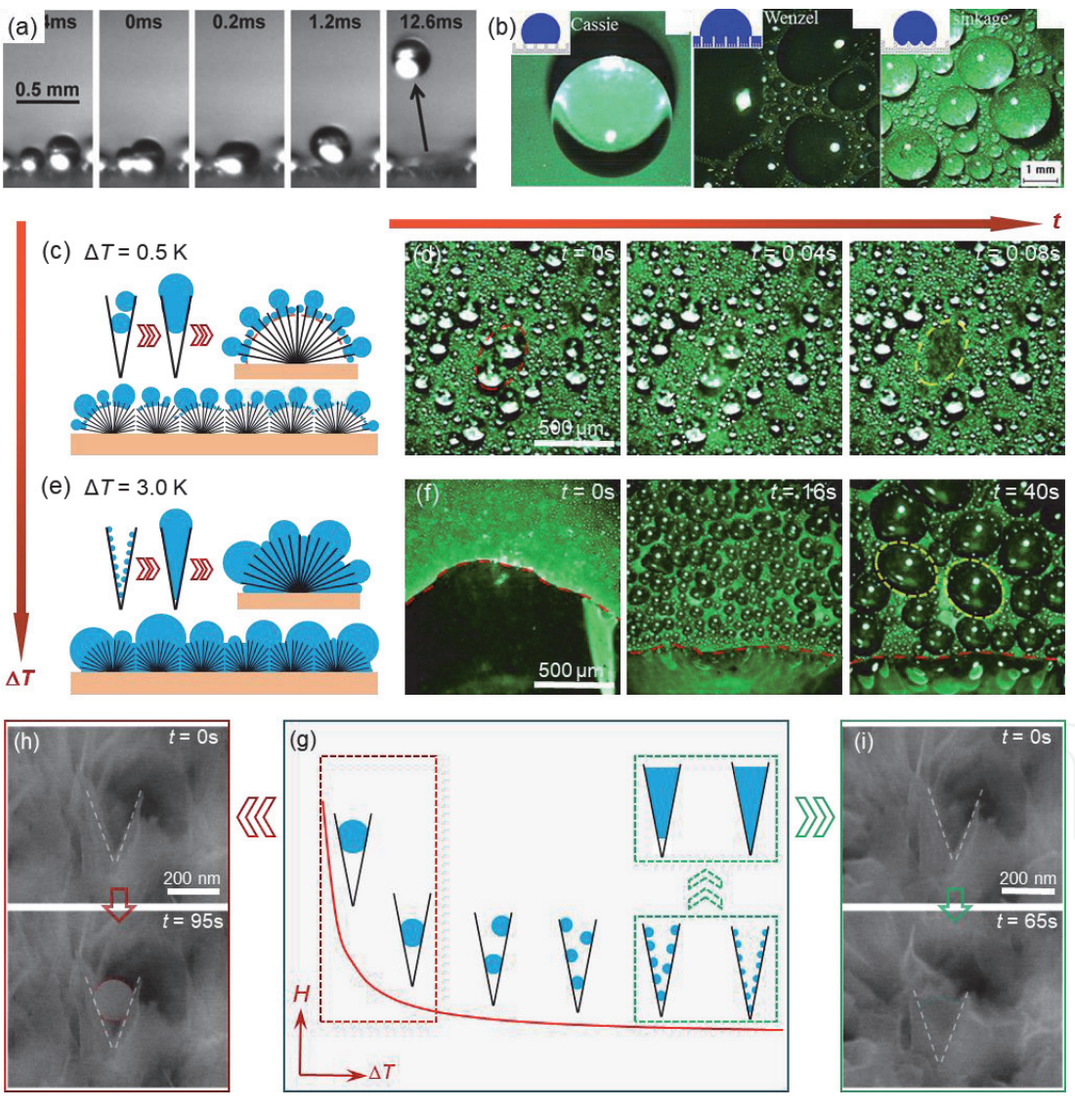

Figure 8.
Wetting and dynamics of the droplet on the superhydrophobic surfaces. (a) Droplet jumping due to the merge of two small droplets [83]. (b) Various wetting modes of condensed droplets on a nanostructured surface [87]. (c–i) Wetting transition of condensed droplets with the increase of surface subcooling: (c) schematic illustrating suspended droplets under a small subcooling, (d) time-lapse images of jumping droplets, (e) schematic illustrating immersed droplets under a large subcooling, (f) time-lapse images of flooding phenomenon, (g) schematic illustrating droplet nucleation in the nanostructure as a function of subcooling. ESEM images of a suspended (h) and immersed (i) droplet in nanostructures at a small and a large surface subcooling, respectively [24].

droplets have been shown to enhance dropwise condensation through accelerating surface refreshing and reducing time-averaged droplet thermal resistance on the surface [22, 66, 85, 86]. Different from the wetting states of the injected droplets on a superhydrophobic surface, such as the millimeter-scale raindrops that are much larger than the micro/nanoscale structure features of lotus leaves, vapor condensation starts with the formation of nanoscale droplets, which can result in loss of non-wettability and flooding phenomenon on micro/nanostructured surfaces. Various droplet wetting modes (**Figure 8b**), for example, Wenzel state, Cassie state, and partially wetting state, have been observed on the superhydrophobic surface [87, 88]. Moreover, the wetting transition of condensed droplets can cause a large degradation of heat transfer performance [22, 89]. A considerable amount of work has focused on understanding the effect of surface structure and wettability on wetting transition with a variety of explanations including surface free energy models [88, 90, 91], Laplace pressure instabilities [92–94], and thermodynamic models [95, 96].

Figure 8c–i shows that the condensation mode transitions from jumping droplet condensation to flooding condensation on a nanostructured superhydrophobic surface as the surface subcooling increases from 0.3 to 3 K [24]. To illustrate the mechanism of wetting transition, a spatial confinement effect on the droplet nucleation was proposed to explain the wetting states of condensed droplets under different surface subcooling. Condensation begins with nucleation with the formation of nanoscale condensed droplets, with the diameter of several nanometers at large subcooling to hundreds of nanometers at small subcooling. Besides, the nucleation site density is inversely proportional to the critical droplet nucleation radius, $N_s \sim 0.037/r_{min}$ [97]. Under a small subcooling, sparse large nucleated droplets on the nanostructures tend to form as the suspended Cassie state (**Figure 8c**), promoting the subsequent self-droplet jumping and effective surface refreshing (**Figure 8d**). As the surface subcooling increases, the critical droplet radius rapidly decreases, leading to the preferred droplet nucleation at the bottom of nanostructures (**Figure 8e**). With the further increase of surface subcooling, large pinned droplets can form on the nanostructures (**Figure 8f**). This is due to the coalescence between a large number of small droplets nucleated within the structures, filling the nanostructures with liquid condensate. To validate the proposed effect of spatial confinement on droplet formation on superhydrophobic surfaces, **Figure 8g,h** shows the experimental observation of the wetting states of nucleated droplets in the nanoscale gaps at different surface subcooling. Small surface subcooling promotes the formation of suspended droplets (**Figure 8h**) due to a larger critical nucleation size (about 166 nm), while large surface subcooling results in the immersed droplet (**Figure 8i**) due to a smaller critical nucleation size. Thus, the wetting states of condensed droplets on the micro/nanostructured surfaces can be controlled by manipulating initial nucleation through adjusting the structure feature and length scale of surface structures.

To delay the occurrence of flooding for achieving stable jumping droplets, various superhydrophobic surfaces with closely spaced nanostructures (**Figure 9a**) have been recently proposed to spatially control nucleation [66, 98, 99]. Minimizing the spacings using high-aspect ratio nanowires can promote to obtain a vapor density difference between the inside and outside of the nanoscale spacing. By this strategy of controlling vapor density, the closely spaced nanowires have been demonstrated to mitigate droplet nucleation in the spacing with a larger energy barrier compared with the top surface of nanowires. The formation of mobile droplets in suspended or partially wetting states is favored for jumping droplet condensation. Compared to the droplet sliding on a plain hydrophobic surface driven by gravity (**Figure 9b**), droplets on the superhydrophobic nanowired surface can be

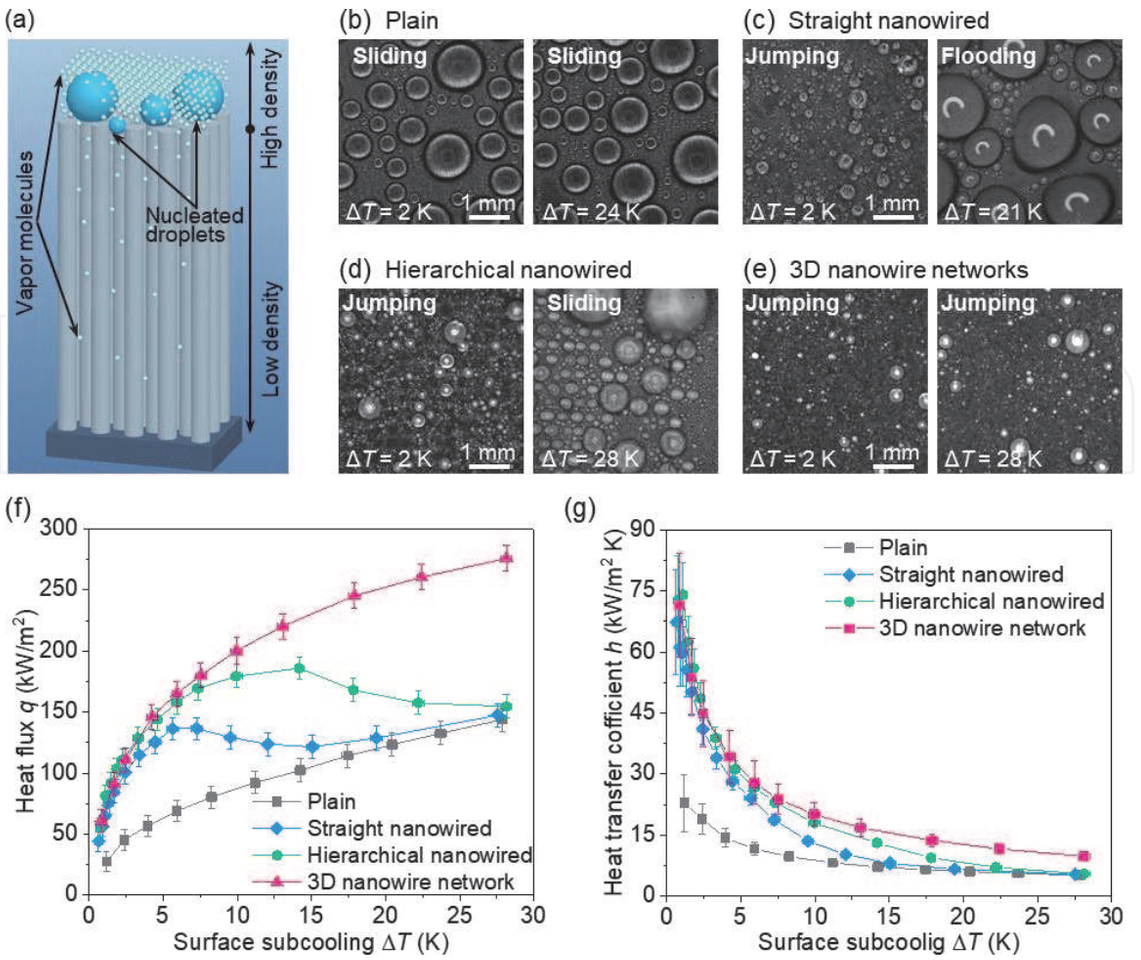

Figure 9.
Superhydrophobic copper nanowires for enhancing condensation heat transfer. (a) Schematic illustrating the spatial control of nucleation for mobile droplets on the top of closely spaced nanowires [66]. (b–e) Droplet behaviors on the plain hydrophobic, straight nanowired, and hierarchical nanowired surfaces, and 3D nanowire networks [67]. (f–g) Heat flux and heat transfer coefficient as a function of surface subcooling. Stable jumping droplet condensation enables the highest heat flux and heat transfer coefficient on the surface with 3D nanowire networks [67].

efficiently removed by efficient jumping (**Figure 9c**) at a small surface subcooling of 2 K. The enhanced condensation heat flux and heat transfer coefficient on the straight nanowired surfaces as a function of surface subcooling have been experimentally demonstrated compared with conventional dropwise condensation on the plain hydrophobic surface (**Figure 9f,g**). However, condensation heat flux reaches its maximum as surface subcooling increases to 6 K and then slightly reduces as surface subcooling is increased to 15 K. Further increase of surface subcooling can increase heat flux monotonically with a similar trend as dropwise condensation on the plain hydrophobic surface. Subsequently, a hierarchical superhydrophobic surface with micro-patterned copper nanowire arrays was developed to improve droplet dynamics [21]. Micro-valleys, consisting of short nanowire arrays between long nanowire arrays, were fabricated to enable spontaneous droplet movement during droplet growing process. For the droplets formed in the micro-valleys, they can rapidly grow on the short nanowire arrays to a critical size where the droplet dimension is comparable to micro-valleys. Further growth of these droplets can push droplet out from the micro-valleys with a Laplace pressure difference between the bottom and top of the droplet, which accelerates droplet re-nucleation and growth.

Although the range of surface subcooling for jumping droplet condensation has been extended by the spatial control of nucleation using the closely arranged

nanowires, droplet wetting transition still occurs on both the uniform and hierarchical nanowired surfaces (**Figure 9c,d**) with the increase of the surface subcooling, resulting in the heat transfer degradation [21, 66]. This is because the active nucleation size decreases with the increase of surface subcooling while the straight nanowires tend to agglomerate and form a large number of micro-defects on the surface in fabrication processes [66, 73]. For condensation on such structured surfaces, vapor prefers to nucleate first in the micro-defects with a smaller energy barrier, resulting in the formation of large pinned droplets and flooding phenomenon [63, 72]. To avoid the agglomeration of straight nanowires, a 3D copper nanowire network fabricated has recently been demonstrated to eliminate the micro-defects between nanowires [67]. Benefiting from the interconnections between the nanowires, the surface morphology of the 3D nanowire network appears to be homogeneous without micro-defects. Compared to the droplet wetting transition on the uniform and hierarchical nanowired surfaces (**Figure 9c,d**), sustainable droplet jumping phenomena is obtained on the superhydrophobic surface with 3D nanowire networks even at a large surface subcooling of 28 K (**Figure 9e**). Benefiting from the formation of suspended and partially wetting droplets, a significant enhancement in heat transfer is realized on the 3D nanowire networks throughout the wide range of surface subcooling experimented (**Figure 9f,g**).

6. Potential strategies for condensation enhancement

In addition to the condensation enhancement on the superhydrophobic surfaces as mentioned above, several other potential strategies and surfaces have recently been proposed to enhance condensation by manipulating droplet behaviors [5, 27, 28, 30, 64, 68, 100–105]. For example, a hybrid structured surface with wettability contrast was proposed to spatially control nucleation, where droplets preferentially form on the hydrophilic region [27]. By confining the hydrophilic regions on the top of the micropillars that are surrounded by superhydrophobic nanowires, such a hybrid surface can achieve both efficient droplet nucleation and jumping removal. Similar design of hybrid micro/nanostructured surfaces with wetting contrast can be found in the literature [64, 106, 107]. The slippery liquid-infused porous surface has been widely studied to promote droplet mobility [5, 28, 108–112]. A hydrophilic directional slippery rough surface was recently fabricated to improve droplet nucleation and removal [5]. Such surface consists of nanotextured directional microgrooves in which the nanotextures alone are infused with hydrophilic liquid lubricant. The surface has hydrophilic surface chemistry, a slippery interface, directional structures, and large surface areas for droplet nucleation and motion. Further experimentation under atmospheric pressure and pure vapor are needed to elucidate the condensation enhancement. Recently, another strategy was presented to enable thin film condensation on a porous superhydrophilic surface with a hydrophobic coating as a nucleation deterrent and energy barrier for the liquid film to propagate above the surface [101, 113, 114]. Further experimental demonstration of heat transfer enhancement of such thin film condensation is needed. It is noted that most of the surfaces mentioned above require precision fabrication, which is difficult to scale up cost-effectively to meet the large area applications.

Some emerging strategies and surface design provide the potential to achieve condensation enhancement by using macrotextures or low-cost commercial materials [68, 100, 103, 104, 115–117]. The plain hybrid surfaces, consisting of plain hydrophilic and hydrophobic regions, were proposed to achieve dropwise-filmwise condensation for reducing the droplet departure size [23, 100, 115, 116, 118–123].

On such a hybrid surface (**Figure 10a**), the growing droplets in the hydrophobic regions are removed when they grow large enough to contact with the liquid film in the hydrophilic regions, resulting in a smaller removal size than that of gravity-driven departure. Another attempt in coupling droplets with a liquid film for enhanced condensation was recently reported on a hierarchical mesh-covered surface [68]. The typical structural feature of the hierarchical mesh-covered surface is composed of an interweaving microchannel network between a superhydrophobic woven mesh layer and a flat substrate, and a large number of micropores among mesh wires (**Figure 10b**). Vapor permeates freely through the mesh layer and condenses on the substrate to form a thin liquid condensate film that is confined in the interconnected channel network. When the condensate film grows out of the micropores due to the increased condensation heat flux, the surrounding liquid condensate can be drained out by the liquid film flow and eventually leaves the superhydrophobic hierarchical mesh-covered surface in the form of gravity-driven falling droplets. The thin liquid film in the interweaving microchannel network not only provides efficient low-thermal resistance condensation interfaces but also continuously transports liquid condensate to be drained out from the substrate.

When the NCG presences in water vapor, condensation performance is highly dependent on the initial nucleation and mass transfer of vapor molecules in the diffusion layer near the condensing surface [103, 124, 125]. A hydrophilic copper surface with interval fluorocarbon-coated hydrophobic bumps to enable falling droplet-enhanced filmwise condensation (**Figure 10c**). Due to the decreased nucleation energy barrier on the hydrophilic regions, water vapor can rapidly nucleate, grow, and form a thin liquid film on the vertical surface. To prevent continuous thickness growth of condensate liquid film along the vertical tube, interval hydrophobic bumps are designed to remove liquid film periodically, which is enabled by the reduction of surface adhesion for condensate liquid on the hydrophobic bumps. More importantly, the condensate liquid departing from the hydrophobic bumps in the form of falling droplets can strongly disturb the NCG diffusion boundary layer. High-performance condensation heat transfer in the presence of NCG was

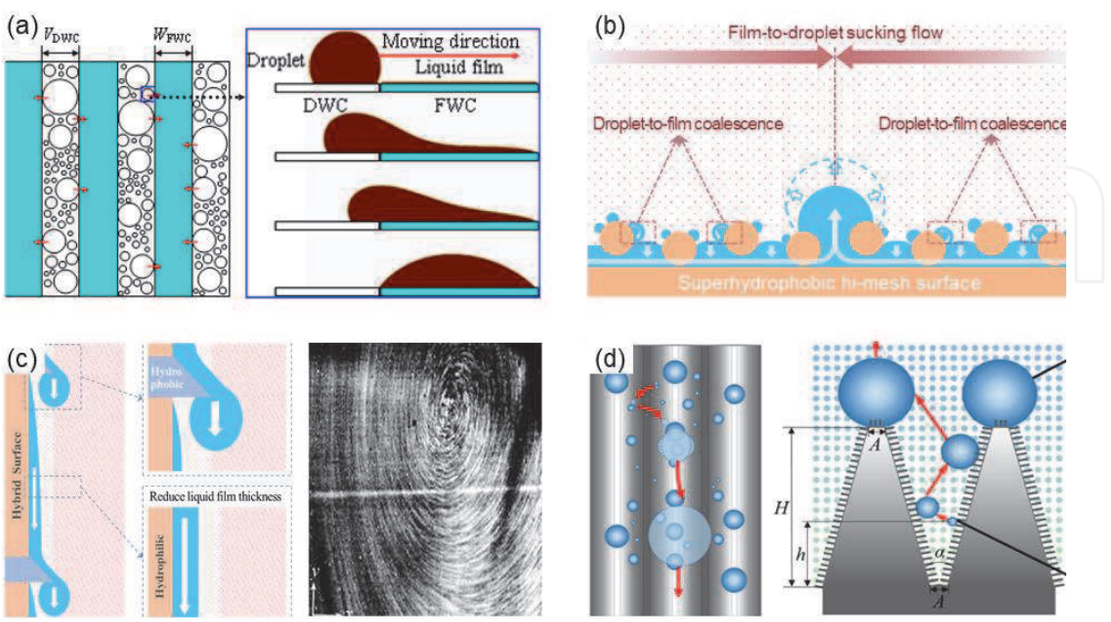

Figure 10.
Emerging strategies and surface design for enhancing condensation heat transfer. (a) Hybrid surface with hydrophobic and hydrophilic stripes to enable dropwise-filmwise condensation [100]. (b) Sucking flow condensation on a hierarchical mesh structured surface [68]. (c) A hydrophilic copper tube surface with interval fluorocarbon-coated hydrophobic bumps [103]. (d) A superhydrophobic surface covered with macrogroove arrays [104].

experimentally demonstrated on the vertical hydrophilic copper tube with hydrophobic fluorocarbon-coated bumps, which is better than both the conventional filmwise and dropwise condensation while avoiding the durability issues of ultrathin hydrophobic coatings. Recently, a structured surface with macrogroove arrays was proposed to improve droplet jumping dynamics in the presence of NCG by coupling rapid droplet growth and efficient droplet jumping relay (**Figure 10d**) [104]. The droplets formed on top of the cones and the bottom of the grooves play different roles during condensation process. Specifically, the cones can promote droplet formation and growth by breaking through the limitation of NCG layer. The droplets with higher mobility can be formed on the bottom of the grooves, resulting in series of coalescence-induced droplet jumping. Such a droplet jumping relay can enable a considerable vibration to trigger the jumping removal of droplets on top of the cones.

7. Summary

This chapter reviewed the recent advances in the fundamental understanding and performance enhancement of dropwise condensation by dancing droplets, as well as some other emerging enhancement strategies and surface design. Various micro/nanostructured surfaces, along with functional wetting coatings, have been developed with designed morphology for diverse surface features. Addressing the intrinsic requirements on multiple length scales in the nucleation, growth, merge/coalescence and departure of the dynamic droplets, unprecedented enhancement in heat transfer performance has been demonstrated for dropwise condensation processes.

An efficient condensing surface should enable both rapid droplet growth and frequent surface refreshing. Due to the excellent surface refreshing capability, jumping droplet condensation on the superhydrophobic surfaces is one of the most active research areas over the last decade on enhancing condensation heat transfer. However, as surface subcooling increases, the mobile droplets in the suspended Cassie state can transition to the highly pinned Wentzel state due to the nucleation occurring within the structures, resulting in the flooding phenomenon and performance degradation. By decreasing the structure scale to be comparable with critical nucleation size, superhydrophobic surfaces with closely spaced nanowires have been demonstrated to minimize droplet nucleation within the structures and to promote the formation of mobile droplets on the surface. On such a nanowired surface, excellent water repellency has been demonstrated to enable efficient jumping droplets without flooding phenomenon, even at a large surface subcooling. A significant enhancement in heat transfer was also achieved under a very wide range of surface subcooling experimented. In addition to the superhydrophobic nanowired surfaces, several other strategies have also been proposed to enhance condensation processes, for example, improving droplet nucleation and jumping by designing hydrophilic patterns on the superhydrophobic surfaces, accelerating droplet removal through liquid film sucking on the hybrid surfaces with hydrophilic and hydrophobic strips, promoting thin film condensation using hybrid nanostructured surfaces, enhancing droplet mobility and transport using slippery liquid-infused porous surfaces, and improving liquid condensate removal using hierarchical mesh-covered surfaces.

Acknowledgements

The authors acknowledge the continuous support from National Natural Science Foundation of China (Nos. 51836002, 51706031, and 51236002), the Fundamental

Research Funds for the Central Universities (No. DUT20RC(3)016), and thank their collaborators who made important contributions to the work reviewed in this chapter including Ronggui Yang, Zhong Lan, Yung-Cheng Lee, Benli Peng, Wei Xu, Sifang Wang.

Conflict of interest

The authors declare no conflict of interest.

Nomenclature

D_{12}	diffusion constant
ΔG_e	nucleation energy, J
h_{fg}	latent heat of vaporization, J/kg
J	nucleation rate
J_0	kinetic constant
k	Boltzmann constant
N	droplet population density, m^{-3}
p_r	vapor pressure, Pa
p_s	saturation pressure, Pa
q_d	heat transfer through individual droplet, W
q	heat flux, W/m^2
r	surface roughness
r_{min}	minimum droplet nucleation radius, m
r_{max}	droplet departure radius, m
Sc	Schmidt number
T	temperature, K
ΔT	surface subcooling, K
U	free-stream velocity, m/s
w	mass transfer flux, mol/m^2
θ	contact angle, °
θ_{adv}	advancing contact angle, °
θ_C	contact angle of Cassie droplet, °
θ_{rec}	receding contact angle, °
θ_W	contact angle of Wenzel droplet, °
$\Delta\theta$	contact angle hysteresis, °
ψ	solid fraction
σ_{lv}	liquid-vapor interfacial tension, N/m
σ_{sv}	solid-vapor interfacial tension, N/m
σ_{sl}	solid-liquid interfacial tension, N/m
μ	kinematic viscosity, $N\ s/m^2$
ρl	liquid density, kg/m^3
$\boldsymbol{\delta_0}$	thickness of boundary layer, m

Author details

Rongfu Wen* and Xuehu Ma*
School of Chemical Engineering, Dalian University of Technology, Dalian, P.R. China

*Address all correspondence to: rongfuwen@dlut.edu.cn and xuehuma@dlut.edu.cn

References

[1] Attinger D, Frankiewicz C, Betz AR, Schutzius TM, Ganguly R, Das A, et al. Surface engineering for phase change heat transfer: A review. MRS Energy & Sustainability. 2014;**1**:1-40

[2] Chen X, Ye H, Fan X, Ren T, Zhang G. A review of small heat pipes for electronics. Applied Thermal Engineering. 2016;**96**:1-17

[3] Stark AK, Klausner JF. An R&D strategy to decouple energy from water. Joule. 2017;**1**:416-420

[4] Urban JJ. Emerging scientific and engineering opportunities within the water-energy nexus. Joule. 2017;**1**(4): 665-688

[5] Dai X, Sun N, Nielsen SO, Stogin BB, Wang J, Yang S, et al. Hydrophilic directional slippery rough surfaces for water harvesting. Science Advances. 2018;**4**(3):eaaq0919

[6] Ni G, Li G, Boriskina L, Svetlana V, Li H, Yang W, et al. Steam generation under one sun enabled by a floating structure with thermal concentration. Nature Energy. 2016;**1**(9):16126

[7] Zhao F, Zhou X, Shi Y, Qian X, Alexander M, Zhao X, et al. Highly efficient solar vapour generation via hierarchically nanostructured gels. Nature Nanotechnology. 2018;**13**(6): 489-495

[8] Yeow JTW, She JPM. Carbon nanotube-enhanced capillary condensation for a capacitive humidity sensor. Nanotechnology. 2006;**17**(21): 5441-5448

[9] Hao T, Wang K, Chen Y, Ma X, Lan Z, Bai T. Multiple bounces and oscillatory movement of a microdroplet in superhydrophobic minichannels. Industrial and Engineering Chemistry Research. 2018;**57**(12):4452-4461

[10] Boreyko JB, Zhao YJ, Chen CH. Planar jumping-drop thermal diodes. Applied Physics Letters. 2011;**99**(23): 234105

[11] Oh J, Birbarah P, Foulkes T, Yin SL, Rentauskas M, Neely J, et al. Jumping-droplet electronics hot-spot cooling. Applied Physics Letters. 2017;**110**(12): 123107

[12] Miljkovic N, Preston DJ, Enright R, Wang EN. Jumping-droplet electrostatic energy harvesting. Applied Physics Letters. 2014;**105**(1):013111

[13] Xu W, Lan Z, Peng BL, Wen RF, Ma XH. Effect of surface free energies on the heterogeneous nucleation of water droplet: A molecular dynamics simulation approach. The Journal of Chemical Physics. 2015;**142**(5):054701

[14] Wen RF, Lan Z, Peng BL, Xu W, Ma XH. Droplet dynamics and heat transfer for dropwise condensation at lower and ultra-lower pressure. Applied Thermal Engineering. 2015;**88**: 265-273

[15] Rose JW. Dropwise condensation theory and experiment: A review. Proceedings of the Institution of Mechanical Engineers, Part A. 2002;**216** (A2):115-128

[16] Lan Z, Wen RF, Wang AL, Ma XH. A droplet model in steam condensation with noncondensable gas. International Journal of Thermal Sciences. 2013;**68**:1-7

[17] Xu W, Lan Z, Peng BL, Wen RF, Ma XH. Evolution of transient cluster/droplet size distribution in a heterogeneous nucleation process. RSC Advances. 2014;**4**(60):31692-31699

[18] Xu W, Lan Z, Peng BL, Wen RF, Ma XH. Heterogeneous nucleation capability of conical microstructures for

water droplets. RSC Advances. 2015; **5**(2):812-818

[19] Varanasi KK, Hsu M, Bhate N, Yang WS, Deng T. Spatial control in the heterogeneous nucleation of water. Applied Physics Letters. 2009;**95**(9): 094101

[20] Miljkovic N, Enright R, Wang EN. Effect of droplet morphology on growth dynamics and heat transfer during condensation on superhydrophobic nanostructured surfaces. ACS Nano. 2012;**6**(2):1776-1785

[21] Wen RF, Xu SS, Zhao DL, Lee YC, Ma XH, Yang RG. Hierarchical superhydrophobic surfaces with micropatterned nanowire arrays for high-efficiency jumping droplet condensation. ACS Applied Materials & Interfaces. 2017;**9**(51):44911-44921

[22] Miljkovic N, Enright R, Nam Y, Lopez K, Dou N, Sack J, et al. Jumping-droplet-enhanced condensation on scalable superhydrophobic nanostructured surfaces. Nano Letters. 2013;**13**(1):179-187

[23] Narhe RD, Beysens DA. Nucleation and growth on a superhydrophobic grooved surface. Physical Review Letters. 2004;**93**(7):076103

[24] Wen RF, Lan Z, Peng BL, Xu W, Yang RG, Ma XH. Wetting transition of condensed droplets on nanostructured superhydrophobic surfaces: Coordination of surface properties and condensing conditions. ACS Applied Materials & Interfaces. 2017;**9**(15): 13770-13777

[25] Mouterde T, Lehoucq G, Xavier S, Checco A, Black CT, Rahman A, et al. Antifogging abilities of model nanotextures. Nature Materials. 2017;**16**: 658-663

[26] Hou Y, Yu M, Shang Y, Zhou P, Song R, Xu X, et al. Suppressing ice nucleation of supercooled condensate with biphilic topography. Physical Review Letters. 2018;**120**(7):075902

[27] Hou YM, Yu M, Chen XM, Wang ZK, Yao SH. Recurrent filmwise and dropwise condensation on a beetle mimetic surface. ACS Nano. 2015;**9**(1): 71-81

[28] Park KC, Kim P, Grinthal A, He N, Fox D, Weaver JC, et al. Condensation on slippery asymmetric bumps. Nature. 2016;**531**(7592):78-82

[29] Rykaczewski K, Paxson AT, Staymates M, Walker ML, Sun XD, Anand S, et al. Dropwise condensation of low surface tension fluids on omniphobic surfaces. Scientific Reports. 2014;**4**:4158

[30] Anand S, Paxson AT, Dhiman R, Smith JD, Varanasi KK. Enhanced condensation on lubricant-impregnated nanotextured surfaces. ACS Nano. 2012; **6**(11):10122-10129

[31] Lafuma A, Quere D. Superhydrophobic states. Nature Materials. 2003;**2**(7):457-460

[32] Maa JR. Drop size distribution and heat-flux of dropwise condensation. Chemical Engineering Journal. 1978; **16**(3):171-176

[33] Ma XH, Song TY, Lan Z, Bai T. Transient characteristics of initial droplet size distribution and effect of pressure on evolution of transient condensation on low thermal conductivity surface. International Journal of Thermal Sciences. 2010; **49**(9):1517-1526

[34] Xu W, Lan Z, Liu Q, Du B, Ma X. Droplet size distributions in dropwise condensation heat transfer: Consideration of droplet overlapping and multiple re-nucleation. International Journal of Heat and Mass Transfer. 2018;**127**:44-54

[35] Kim S, Kim KJ. Dropwise condensation modeling suitable for superhydrophobic surfaces. Journal of Heat Transfer. 2011;**133**(8):081502

[36] Ma XH, Rose JW, Xu DQ, Lin JF, Wang BX. Advances in dropwise condensation heat transfer: Chinese research. Chemical Engineering Journal. 2000;**78**(2–3):87-93

[37] Wen RF, Lan Z, Peng BL, Xu W, Ma XH, Cheng YQ. Droplet departure characteristic and dropwise condensation heat transfer at low steam pressure. Journal of Heat Transfer. 2016; **138**:071501

[38] Le Ferve EJ, Rose JW. A theory of heat transfer by dropwise condensation. In: Proceedings of the Third International Heat Transfer Conference. Chicago, IL: American Institute of Chemical Engineers; 1966. pp. 362-375

[39] AbuOrabi M. Modeling of heat transfer in dropwise condensation. International Journal of Heat and Mass Transfer. 1998;**41**(1):81-87

[40] Miljkovic N, Enright R, Wang EN. Modeling and optimization of superhydrophobic condensation. Journal of Heat Transfer. 2013;**135**(11): 111004

[41] Vemuri S, Kim KJ. An experimental and theoretical study on the concept of dropwise condensation. International Journal of Heat and Mass Transfer. 2006;**49**(3–4):649-657

[42] Lee S, Yoon HK, Kim KJ, Kim S, Kennedy M, Zhang BJ. A dropwise condensation model using a nano-scale, pin structured surface. International Journal of Heat and Mass Transfer. 2013;**60**:664-671

[43] Liu X, Cheng P. Dropwise condensation theory revisited part II. Droplet nucleation density and condensation heat flux. International Journal of Heat and Mass Transfer. 2015; **83**:842-849

[44] Zheng S, Eimann F, Philipp C, Fieback T, Gross U. Modeling of heat and mass transfer for dropwise condensation of moist air and the experimental validation. International Journal of Heat and Mass Transfer. 2018;**120**:879-894

[45] Niu D, Guo L, Hu HW, Tang GH. Dropwise condensation heat transfer model considering the liquid-solid interfacial thermal resistance. International Journal of Heat and Mass Transfer. 2017;**112**:333-342

[46] Shang Y, Hou Y, Yu M, Yao S. Modeling and optimization of condensation heat transfer at biphilic interface. International Journal of Heat and Mass Transfer. 2018;**122**:117-127

[47] Chavan S, Cha H, Orejon D, Nawaz K, Singla N, Yeung YF, et al. Heat transfer through a condensate droplet on hydrophobic and nanostructured superhydrophobic surfaces. Langmuir. 2016;**32**(31): 7774-7787

[48] Phadnis A, Rykaczewski K. The effect of Marangoni convection on heat transfer during dropwise condensation on hydrophobic and omniphobic surfaces. International Journal of Heat and Mass Transfer. 2017;**115**:148-158

[49] Tanaka H. A theoretical study of dropwise condensation. Journal of Heat Transfer. 1975;**97**(1):72

[50] Mei MF, Yu BM, Cai JC, Luo L. A fractal analysis of dropwise condensation heat transfer. International Journal of Heat and Mass Transfer. 2009;**52**(21–22):4823-4828

[51] Weisensee PB, Wang Y, Qian H, Daniel S, William PK, Miljkovic N. Condensate droplet size distribution on lubricant-infused surfaces. International

Journal of Heat and Mass Transfer. 2017; **109**:187-199

[52] Kulinich SA, Farzaneh M. Hydrophobic properties of surfaces coated with fluoroalkylsiloxane and alkylsiloxane monolayers. Surface Science. 2004;**573**(3):379-390

[53] KKS L, Bico J, KBK T, Chhowalla M, GAJ A, Milne WI, et al. Superhydrophobic carbon nanotube forests. Nano Letters. 2003;**3**:1701-1705

[54] Gnanappa AK, O'Murchu C, Slattery O, Peters F, Aszalós-Kiss B, Tofail SAM. Effect of annealing on hydrophobic stability of plasma deposited fluoropolymer coatings. Polymer Degradation and Stability. 2008;**93**(12):2119-2126

[55] Paxson AT, Yague JL, Gleason KK, Varanasi KK. Stable dropwise condensation for enhancing heat transfer via the initiated chemical vapor deposition (iCVD) of grafted polymer films. Advanced Materials. 2014;**26**(3): 418-423

[56] Preston DJ, Mafra DL, Miljkovic N, Kong J, Wang EN. Scalable graphene coatings for enhanced condensation heat transfer. Nano Letters. 2015;**15**(5): 2902-2909

[57] Azimi G, Dhiman R, Kwon HM, Paxson AT, Varanasi KK. Hydrophobicity of rare-earth oxide ceramics. Nature Materials. 2013;**12**(4): 315-320

[58] Khalil K, Soto D, Paxson A, Katmis AU, Gleason K, Varanasi KK. Grafted nanofilms promote dropwise condensation of low-surface-tension fluids for high-performance heat exchangers. Joule. 2019;**3**(5):1377-1388

[59] McCarthy M, Gerasopoulos K, Maroo SC, Hart AJ. Materials, fabrication, and manufacturing of micro/nanostructured surfaces for phase-change heat transfer enhancement. Nanoscale and Microscale Thermophysical Engineering. 2014; **18**(3):288-310

[60] Lundy R, Byrne C, Bogan J, Nolan K, Collins MN, Dalton E, et al. Exploring the role of adsorption and surface state on the hydrophobicity of rare earth oxides. ACS Applied Materials & Interfaces. 2017;**9**(15): 13751-13760

[61] Fu S-P, Rossero J, Chen C, Li D, Takoudis CG, Abiade JT. On the wetting behavior of ceria thin films grown by pulsed laser deposition. Applied Physics Letters. 2017;**110**(8): 081601

[62] Cha H, Wu A, Kim MK, Saigusa K, Liu A, Miljkovic N. Nanoscale-agglomerate-mediated heterogeneous nucleation. Nano Letters. 2017;**17**(12): 7544-7551

[63] Lo CW, Wang CC, Lu MC. Scale effect on dropwise condensation on superhydrophobic surfaces. ACS Applied Materials & Interfaces. 2014; **6**(16):14353-14359

[64] Chen XM, Wu J, Ma RY, Hua M, Koratkar N, Yao SH, et al. Nanograssed micropyramidal architectures for continuous dropwise condensation. Advanced Functional Materials. 2011; **21**(24):4617-4623

[65] Anderson DM, Gupta MK, Voevodin AA, Hunter CN, Putnam SA, Tsukruk VV, et al. Using amphiphilic nanostructures to enable long-range ensemble coalescence and surface rejuvenation in dropwise condensation. ACS Nano. 2012;**6**(4):3262-3268

[66] Wen RF, Li Q, Wu JF, Wu GS, Wang W, Chen YF, et al. Hydrophobic copper nanowires for enhancing condensation heat transfer. Nano Energy. 2017;**33**:177-183

[67] Wen RF, Xu SS, Ma XH, Lee YC, Yang RG. Three-dimensional superhydrophobic nanowire networks for enhancing condensation heat transfer. Joule. 2018;**2**(2):269-279

[68] Wen R, Xu S, Zhao D, Yang L, Ma X, Liu W, et al. Sustaining enhanced condensation on hierarchical mesh-covered surfaces. National Science Review. 2018;**5**(6):878-887

[69] Roach P, Shirtcliffe NJ, Newton MI. Progess in superhydrophobic surface development. Soft Matter. 2008;**4**(2): 224-240

[70] Lu MC, Chen R, Srinivasan V, Carey VP, Majumdar A. Critical heat flux of pool boiling on Si nanowire array-coated surfaces. International Journal of Heat and Mass Transfer. 2011; **54**(25–26):5359-5367

[71] Li Y, Duan C. Bubble-regulated silicon nanowire synthesis on micro-structured surfaces by metal-assisted chemical etching. Langmuir. 2015; **31**(44):12291-12299

[72] Lo CW, Wang CC, Lu MC. Spatial control of heterogeneous nucleation on the superhydrophobic nanowire array. Advanced Functional Materials. 2014; **24**(9):1211-1217

[73] Wen RF, Li Q, Wang W, Latour B, Li CH, Li C, et al. Enhanced bubble nucleation and liquid rewetting for highly efficient boiling heat transfer on two-level hierarchical surfaces with patterned copper nanowire arrays. Nano Energy. 2017;**38**:59-65

[74] Lan Z, Chen F, Qiang W, Xue Q, Ma X. Direct observation of water clusters for surface design. Chemical Engineering Science. 2020;**217**:115475

[75] Xu W, Lan Z, Peng BL, Wen RF, Ma XH. Effect of nano structures on the nucleus wetting modes during water vapour condensation: From individual groove to nano-array surface. RSC Advances. 2016;**6**(10):7923-7932

[76] Peng BL, Wang SF, Lan Z, Xu W, Wen RF, Ma XH. Analysis of droplet jumping phenomenon with lattice Boltzmann simulation of droplet coalescence. Applied Physics Letters. 2013;**102**(15):151601

[77] Huang D, Quan X, Cheng P. An investigation on vapor condensation on nanopillar array surfaces by molecular dynamics simulation. International Journal of Heat and Mass Transfer. 2018;**98**:232-238

[78] Liu X, Cheng P, Quan X. Lattice Boltzmann simulations for self-propelled jumping of droplets after coalescence on a superhydrophobic surface. International Journal of Heat and Mass Transfer. 2014;**73**:195-200

[79] Niu D, Tang G. Molecular dynamics simulation of droplet nucleation and growth on a rough surface: Revealing the microscopic mechanism of the flooding mode. RSC Advances. 2018; **8**(43):24517-24524

[80] Gao S, Liao Q, Liu W, Liu Z. Effects of solid fraction on droplet wetting and vapor condensation: A molecular dynamic simulation study. Langmuir. 2017;**33**:12379-12388

[81] Zhang L, Xu Z, Lu Z, Du J, Wang EN. Size distribution theory for jumping-droplet condensation. Applied Physics Letters. 2019;**114**:163701

[82] Mei MF, Hu F, Han C, Cheng Y. Time-averaged droplet size distribution in steady-state dropwise condensation. International Journal of Heat and Mass Transfer. 2015;**88**:338-345

[83] Boreyko JB, Chen CH. Self-propelled dropwise condensate on superhydrophobic surfaces. Physical Review Letters. 2009;**103**(18):184501

[84] Yan X, Zhang L, Sett S, Feng L, Zhao C, Huang Z, et al. Droplet jumping: Effects of droplet size, surface structure, pinning, and liquid properties. ACS Nano. 2019;**13**(2): 1309-1323

[85] Preston DJ, Wang EN. Jumping droplets push the boundaries of condensation heat transfer. Joule. 2018; **2**(2):205-207

[86] Enright R, Miljkovic N, Alvarado JL, Kim K, Rose JW. Dropwise condensation on micro- and nanostructured surfaces. Nanoscale and Microscale Thermophysical Engineering. 2014;**18**(3):223-250

[87] Ma XH, Wang SF, Lan Z, Peng BL, Ma HB, Cheng P. Wetting mode evolution of steam dropwise condensation on superhydrophobic surface in the presence of noncondensable gas. Journal of Heat Transfer. 2012;**134**(2):021501

[88] Enright R, Miljkovic N, Al-Obeidi A, Thompson CV, Wang EN. Condensation on superhydrophobic surfaces: The role of local energy barriers and structure length scale. Langmuir. 2012;**28**(40):14424-14432

[89] Zhang P, Maeda Y, Lv F, Takata Y, Orejon D. Enhanced coalescence-induced droplet-jumping on nanostructured superhydrophobic surfaces in the absence of microstructures. ACS Applied Materials & Interfaces. 2017;**9**(40):35391-35403

[90] Xu W, Lan Z, Peng BL, Wen RF, Chen YS, Ma XH. Directional movement of droplets in grooves: Suspended or immersed? Scientific Reports. 2016;**6**:18836

[91] Rykaczewski K, Paxson AT, Anand S, Chen XM, Wang ZK, Varanasi KK. Multimode multidrop serial coalescence effects during condensation on hierarchical superhydrophobic surfaces. Langmuir. 2013;**29**(3):881-891

[92] Park KC, Choi HJ, Chang CH, Cohen RE, McKinley GH, Barbastathis G. Nanotextured silica surfaces with robust superhydrophobicity and omnidirectional broadband supertransmissivity. ACS Nano. 2012; **6**(5):3789-3799

[93] Checco A, Ocko BM, Rahman A, Black CT, Tasinkevych M, Giacomello A, et al. Collapse and reversibility of the superhydrophobic state on nanotextured surfaces. Physical Review Letters. 2014;**112**(21):216101

[94] Feng J, Qin ZQ, Yao SH. Factors affecting the spontaneous motion of condensate drops on superhydrophobic copper surfaces. Langmuir. 2012;**28**(14): 6067-6075

[95] Raj R, Enright R, Zhu YY, Adera S, Wang EN. Unified model for contact angle hysteresis on heterogeneous and superhydrophobic surfaces. Langmuir. 2012;**28**(45):15777-15788

[96] Rykaczewski K, Osborn WA, Chinn J, Walker ML, Scott JHJ, Jones W, et al. How nanorough is rough enough to make a surface superhydrophobic during water condensation? Soft Matter. 2012;**8**(33):8786-8794

[97] Rose JW. Further aspects of dropwise condensation theory. International Journal of Heat and Mass Transfer. 1976;**19**(12):1363-1370

[98] Seo D, Shim J, Moon B, Lee K, Lee J, Lee C, et al. Passive anti-flooding superhydrophobic surfaces. ACS Applied Materials & Interfaces. 2020; **12**(3):4068-4080

[99] Xing D, Wu F, Wang R, Zhu J, Gao X. Microdrop-assisted microdomain hydrophilicization of superhydrophobic surfaces for

high-efficiency nucleation and self-removal of condensate microdrops. ACS Applied Materials & Interfaces. 2019; **11**(7):7553-7558

[100] Peng BL, Ma XH, Lan Z, Xu W, Wen RF. Experimental investigation on steam condensation heat transfer enhancement with vertically patterned hydrophobic-hydrophilic hybrid surfaces. International Journal of Heat and Mass Transfer. 2015;**83**:27-38

[101] Oh J, Zhang R, Shetty PP, Krogstad JA, Braun PV, Miljkovic N. Thin film condensation on nanostructured surfaces. Advanced Functional Materials. 2018;**28**:1707000

[102] Yao Y, Aizenberg J, Park K-C. Dropwise condensation on hydrophobic bumps and dimples. Applied Physics Letters. 2018;**112**(15):151605

[103] Wen R, Zhou X, Peng B, Lan Z, Yang R, Ma X. Falling-droplet-enhanced filmwise condensation in the presence of non-condensable gas. International Journal of Heat and Mass Transfer. 2019;**140**:173-186

[104] Cheng Y, Du B, Wang K, Chen Y, Lan Z, Wang Z, et al. Macrotextures-induced jumping relay of condensate droplets. Applied Physics Letters. 2019; **114**(9):093704

[105] Bintein P-B, Lhuissier H, Mongruel A, Royon L, Beysens D. Grooves accelerate dew shedding. Physical Review Letters. 2019;**122**(9): 098005

[106] Mondal B, Mac Giolla Eain M, Xu Q, Egan VM, Punch J, Lyons AM. Design and fabrication of a hybrid superhydrophobic-hydrophilic surface that exhibits stable dropwise condensation. ACS Applied Materials & Interfaces. 2015;**7**(42):23575-23588

[107] Tang Z, He M, Bian R, Duan Z, Luan K, Hou J, et al. Multiple superwettable nanofiber arrays prepared by a facile dewetting strategy via controllably localizing a low-energy compound. Advanced Functional Materials. 2019;**29**(30):1900060

[108] Hao C, Li J, Liu Y, Zhou X, Liu Y, Liu R, et al. Superhydrophobic-like tunable droplet bouncing on slippery liquid interfaces. Nature Communications. 2015;**6**:7986

[109] Preston DJ, Lu Z, Song Y, Zhao Y, Wilke KL, Antao DS, et al. Heat transfer enhancement during water and hydrocarbon condensation on lubricant infused surfaces. Scientific Reports. 2018;**8**(1):540

[110] Seo D, Shim J, Lee C, Nam Y. Brushed lubricant-impregnated surfaces (BLIS) for long-lasting high condensation heat transfer. Scientific Reports. 2020;**10**(1):2959

[111] Sett S, Sokalski P, Boyina K, Li L, Rabbi KF, Auby H, et al. Stable dropwise condensation of ethanol and hexane on rationally designed ultrascalable nanostructured lubricant-infused surfaces. Nano Letters. 2019; **19**(8):5287-5296

[112] Jing X, Guo Z. Durable lubricant impregnated surfaces for water collection under extremely severe working conditions. ACS Applied Materials & Interfaces. 2019;**11**(39): 35949-35958

[113] Preston DJ, Wilke KL, Lu Z, Cruz SS, Zhao Y, Becerra LL, et al. Gravitationally driven wicking for enhanced condensation heat transfer. Langmuir. 2018;**34**(15):4658-4664

[114] Wang R, Antao DS. Capillary-enhanced filmwise condensation in porous media. Langmuir. 2018;**34**: 13855-13863

[115] Alwazzan M, Egab K, Peng B, Khan J, Li C. Condensation on hybrid-

patterned copper tubes (I): Characterization of condensation heat transfer. International Journal of Heat and Mass Transfer. 2017;**112**:991-1004

[116] Winter RL, McCarthy M. Dewetting from amphiphilic minichannel surfaces during condensation. ACS Applied Materials & Interfaces. 2020;**12**(6):7815-7825

[117] Cheng Y, Wang Z. New approach for efficient condensation heat transfer. National Science Review. 2019;**6**(2): 185-186

[118] Peng BL, Ma XH, Lan Z, Xu W, Wen RF. Analysis of condensation heat transfer enhancement with dropwise-filmwise hybrid surface: Droplet sizes effect. International Journal of Heat and Mass Transfer. 2014;**77**:785-794

[119] Wu J, Zhang L, Wang Y, Wang P. Efficient and anisotropic fog harvesting on a hybrid and directional surface. Advanced Materials Interfaces. 2017; **4**(2):1600801

[120] Yang K-S, Huang Y-Y, Liu Y-H, Wu S-K, Wang C-C. Enhanced dehumidification via hybrid hydrophilic/hydrophobic morphology having wedge gradient and drainage channels. Heat and Mass Transfer. 2019; **55**:3359-3368

[121] Gou X, Guo Z. Hybrid hydrophilic-hydrophobic CuO@TiO2-coated copper mesh for efficient water harvesting. Langmuir. 2020;**36**(1):64-73

[122] Sharma CS, Lam CWE, Milionis A, Eghlidi H, Poulikakos D. Self-sustained cascading coalescence in surface condensation. ACS Applied Materials & Interfaces. 2019;**11**(30):27435-27442

[123] Boreyko JB, Hansen RR, Murphy KR, Nath S, Retterer ST, Collier CP. Controlling condensation and frost growth with chemical micropatterns. Scientific Reports. 2016; **6**:19131

[124] Ma XH, Zhou XD, Lan Z, Li YM, Zhang Y. Condensation heat transfer enhancement in the presence of non-condensable gas using the interfacial effect of dropwise condensation. International Journal of Heat and Mass Transfer. 2008;**51**(7–8):1728-1737

[125] Zhao Y, Preston DJ, Lu Z, Zhang L, Queeney J, Wang EN. Effects of millimetric geometric features on dropwise condensation under different vapor conditions. International Journal of Heat and Mass Transfer. 2018;**119**: 931-938